Chapter 5

Simulated Quadrant Photodiode

5.1 Introduction

As demonstrated in Chapter 3, the motion and behaviour of a dimer is significantly different compared to that of a traditional sphere. While this is simple enough to demonstrate in a simulation, where the position and orientation can be computed using the finite differences method, from an experimental perspective these details can go unnoticed. In order to accurately capture the dynamics of a trapped sphere, a position detection system is typically used - the most common of which is a Quadrant Photo Diode (QPD). A QPD sends a signal measuring the voltage difference between 4 photo diode quadrants. For purely translational motion the diodes can be split into neighbouring pairs (i.e. left and right, top and bottom - see Fig 5.1) to estimate the total displacement made by the target particle. However the same method cannot be applied to stochastic rotational motion.

The relationship between particle translations and light scattering was first demonstrated by Rohrbach, where they showed a linear change in the scattered light when the particle was displaced [4]. They further showed that the optical force exerted by the trapping beam could be determined from the change in scattered light [4]. Rohrbach's model would later be used to develop modern position detection systems, where by calibrating the scattering signal using one of the many calibration techniques one could achieve a highly accurate estimation of the translational motion in the X-Y plane.The

most common of which being the Power Spectral Density method, one of the greatest advantages of the PSD method is that periodic rotational motion is also captured in the power spectrum. As an example consider an elongated cylindrical particle that is wobbling around the Z-axis at some periodic frequency 'f'. A power spectrum of that trajectory will show a peak at that frequency. If however the wobble is periodic but instead stochastic, then it is impossible to separate out the rotational motion from the translational motion. This poses some challenges to experimental modelling of non-spherical particles, if we cannot glean any information on the orientation of the trapped particle we cannot accurately distinguish between sphere's and dimers

As a solution we developed a model similar to that of Rohrbach's but now utilising a *mstm* to provide the light scattering for a dimer. We begin with a brief discussion of the working principle behind a position detection device. We then provide a framework for replicating the scattering signal recorded by a quadrant photo diode. We show that extending the framework to capture information from an arbitrary shaped particle is simple in principle but difficult to interpret, we demonstrate as such by comparing the expected signal from a trapped sphere, to that of a trapped dimer.

5.1.1 Position Detection methods

Here we discuss how one can record a trajectory using a QPD and use it to interpret the particle's real time motion. The QPD is constructed of four photo diodes assembled in a quadrant formation, when a particle is trapped the interference pattern produced is focused onto the QPD, with the maximum intensity mapping to the particle's centre of mass. By summing the voltages of the horizontal and vertical quadrants together the particle's centre of mass is tracked in the $x - y$ plane. Axial displacement can be estimated by observing the change in the total voltage of the QPD. The outputted signal gives an indication of the particle's relative displacement from the beam focus, but in order to convert the signal to distance units the trap needs to be calibrated (assuming a linear response curve).

Now while the signal returned by the QPD is proportional to the particle's displacement it cannot be directly interpreted as such until converted from voltage units

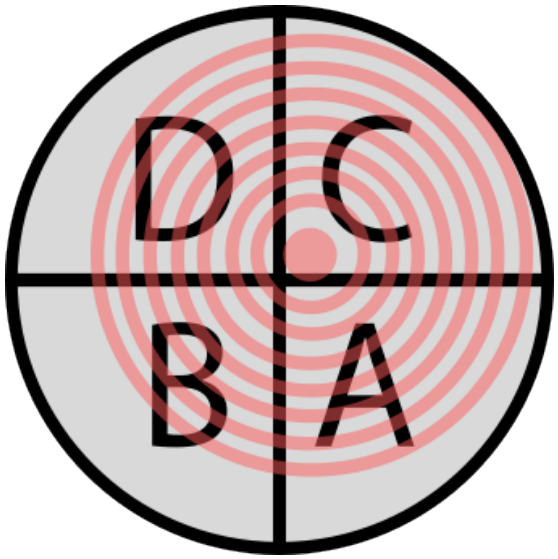

Figure 5.1: Diagram depicting a typical QPD interface. The four quadrants of a QPD experience different photocurrents based on the total intensity of light incident on each section (labelled A, B, C, D).

to displacement units. This can be done by taking the ratio of the expected diffusion coefficient D_{exp} and the diffusion coefficient calculated by calibration D_{cal}.

$$D_{exp} = \frac{k_B T}{6\pi\eta a} \Rightarrow Conversion\ Factor\ [m/V] = \sqrt{\frac{D_{ext}}{D_{cal}}} \tag{5.1}$$

The former depends on the exact size and shape of the target particle, using image analysis one can get a fairly accurate estimation of the particles radius (a). The latter can be determined from fitting the QPD signal to a given model, for computing the diffusion coefficient computing the auto correlation function, the mean square displacement, or taking the power spectrum are used. The former two are ideal for simple position detection systems, where the QPD reports the signal at each time step, however they often require longer recording times in order to reach an ideal accuracy. More sophisticated QPD systems can calculate the power spectra of an incoming signal and immediately fit it to a power spectrum. Once the conversion factor is known any further QPD signals can be converted immediately into displacement units to monitor the position of the target particle, the spacial resolution being limited by the accuracy of the calibration method. A full tutorial in maximising the accuracy of the power

spectral method is provided by Berg and Sorensen [1]

For our consideration we will be relying on the power spectrum method to characterise the motion of the trapped particle. Firstly because it is sometimes integrated into QPD systems. And secondly, because on of the main advantages of the power spectrum method is its shorter calibration times, and the ability to filter out large sources of signal noise.

5.2 Modelling the QPD response signal of a non-spherical particle

In order to simulate a typical experimental set up with a QPD installed as a position detection system we need to evaluate the total magnitude of the electric field incident on the photo-diode surface. While trapping a micro-particle, the scattered and incident fields combine together and interfere with one another. These fields are collected by a condenser lens in the far field limit and are focused onto the QPD surface, the total intensity can be evaluated as:

$$I(x,y) = \epsilon_0 c \left| \begin{bmatrix} E_{i,x}(x,y) + E_{s,x}(x,y) \\ E_{i,y}(x,y) + E_{s,y}(x,y) \\ E_{i,z}(x,y) + E_{s,z}(x,y) \end{bmatrix} \right|^2 \times step(\theta_{NA} - \theta(x,y)) \tag{5.2}$$

The last term is simply a representative step term that defines the outer limit by which we evaluate the electric field, this is analogous to a condenser lens removing noise from other light sources by only accepting light at a specific acceptance angle defined by its numerical aperture NA_c. Depending on the relative size of our particle we can adjust the acceptance angle, this has very little effect on the transverse signals, but for axial evaluations of a trapped particle the numerical aperture should be tuned so that the resultant response curve has negative slope in order to allow for axial position detection, the method for finding this angle θ_Θ is discussed in [2].

The incident beam is simple enough to define given our set up parameters, for the sake of simplicity we assume that our beam is a Gaussian beam. *Ott* uses a point

matching approach to approximate the beam shape coefficients of the incident field by fitting it to the far field estimate. From the QPD's perspective it is receiving light both from the incident and scattered beam simultaneously, as such both fields must be expressed using outgoing vector spherical harmonics.

$$E_{\text{inc}}(r) = E_0 \sum_{n}^{\infty} \sum_{m=-n}^{n} \left[a_{mn} \mathbf{M}_{nm}^{(2)}(\mathbf{r}) + b_{nm} \mathbf{N}_{nm}^{(2)}(\mathbf{r}) \right] \tag{5.3}$$

$$E_{\text{scat}}(r) = E_0 \sum_{n}^{\infty} \sum_{m=-n}^{n} \left[p_{nm} \mathbf{N}_{nm}^{(2)}(\mathbf{r}) + q_{nm} \mathbf{M}_{nm}^{(2)}(\mathbf{r}) \right] \tag{5.4}$$

Where the superscript (2) denotes an outgoing spherical harmonic function. In order to compute the scattering from the target particle *ott* uses the T-matrix method, this is not essential for a simple sphere but is essential for complex shaped particles such as dimers. The scattered and incident fields are then combined together in the far field to get $I(x, y)$, the quadrant and overall signals are calculated via:

$$Q_i = \sum_{n,m} I(x_{i,n}, y_{i,m}) \tag{5.5}$$

$$S_x = \frac{(Q_1 + Q_2) - (Q_3 + Q_4)}{\sum I_0(x, y)} \tag{5.6}$$

$$S_y = \frac{(Q_1 + Q_3) - (Q_2 + Q_4)}{\sum I_0(x, y)} \tag{5.7}$$

$$S_z = \frac{(Q_1 + Q_2 + Q_3 + Q_4}{\sum I_0(x, y)} \tag{5.8}$$

Where the denominator is the total intensity on the QPD while there is no particle within the trap. You would expect that S_x and S_y are near identical for equal particle displacements, however due to the polarisation of the beam there will be a slight bias to the signals for motion along the direction of the polarisation vector. This is generally not an issue if the particle trajectory is sampled for a long enough time period. By converting from signal units to length units (see Eq.(5.1)) the trap shape can be discerned from the QPD signals, assuming the fluid properties are known to a high degree of accuracy.

While translational motion has no knock on effects to the QPD signal, rotational

changes are double counted by both the incident and total field. This results in rotational motion being biased in the QPD signal - even when collecting signals from isotropic scatterers. To prevent this we rotate the total field via the inverse rotation matrix of the dimer.

To confirm that our method is producing accurate results, we ran a comparison test between our simulative QPD and the results from [4]. Where a 300 nm diameter sphere is scanned across the path of a focused Gaussian beam ($\lambda = 1064\ nm$, $NA = 1.2$), the sphere has a refractive index of 1.57 and is suspended in water ($n_{med} = 1.33$) and the condenser lens has its numerical aperture set to 0.5 ($\theta_{max} = 30°$). Scanning across all three primary axis produced the following response curve:

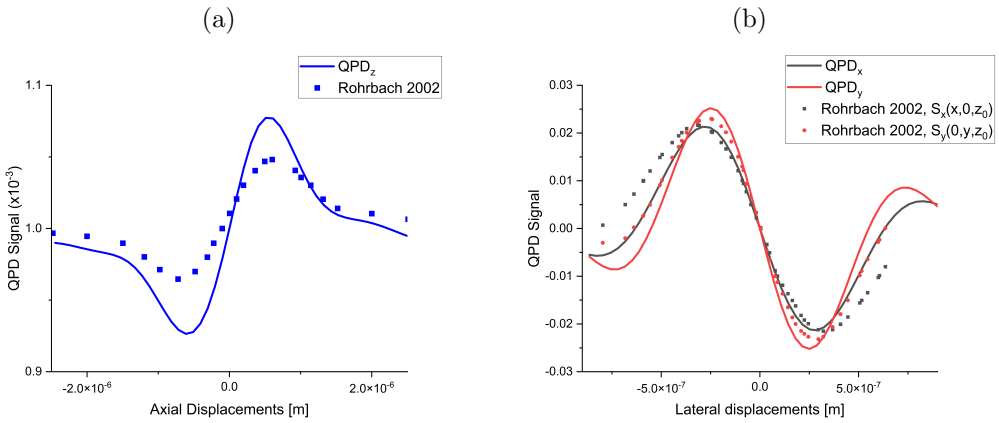

Figure 5.2: Comparison between QPD response signal versus work conducted by Rohrbach, single sphere ($r = 150\ nm$, $n = 1.57$) is scanned by a 1064 nm laser and the QPD signal recorded. Solid lines represent the signal produced by QPD using *ott* and points represent the signal response collected from [4].

The discrepancy between our simulated QPD and the results from Rohrbach can be attributed to the fact that the position to signal error grows as you move further from trap focus. As the particle moves further from the trap focus the error in the attributed signal grows substantially [4]. In most optical trapping experiments we usually are calibrating a strong trap where the mean square displacement falls well within the linear regime shown in fig. 5.2. In which case the error between Rohrbach's model and our own is inconsequential for calibration purposes.

5.3 Characterisation of asymmetric dimer dynamics via PSD analysis

While it is possible to extract all of the relevant dynamics from a simulation, from an experimental standpoint characterising those dynamics is dependent on what experimental techniques are used. Translational motion can be characterised via a position detection system but angular motion is far more difficult to detect, let along characterise.

The tweezer setup we are simulating incorporates a dual objective configuration, using one objective lens to focus the beam (NA=1.25) where as the condenser lens acts as a means of truncating the electric field ($NA_c = 0.25$). The electric field falling onto the QPD surface is computed by considering the far field of the combined incident and scattered beams. We can ignore any contributions from the electric field that falls outwith the maximum acceptance angle of our condenser lens ($\theta_{max} \approx \pm 10.8\,\mathrm{deg}$). This is not perfectly analogous of a true QPD as external factors (i.e. internal resistance, external light sources, and vibrations) would also contribute to the detected QPD signal. It does provide us a means of showing what elements of a particle's trajectory are represented in the power spectrum and which elements are obscured.

As a benchmark we start by considering a single sphere within an optical trap. A single polystyrene sphere suspended in water ($a = 1\mu m$, $n_p = 1.59$, $n_m = 1.33$) was trapped by a focused Gaussian beam ($NA = 1.25$) using circularly polarised light. For the sake of time efficiency the trajectory was sampled every 10 time steps, meaning the upper bound on the power spectra is $f_{Nyq} = f_{sample}/2 = 5000\ Hz$. To optimise the frequency window we fitted the power spectra using the aliased Lorentzian. (Eq. (**??**)).

As shown in fig. 5.3, the two power spectra report different corner frequencies which would be indicate that the trap is not perfectly circular. We can use both *ott* and the trajectory itself to derive an estimation of the trap geometry. Additionally, we fitted the same Lorentzian to the sphere's positional data, this would be a situation when the QPD signals are completely uncorrelated with one another and there is a constant

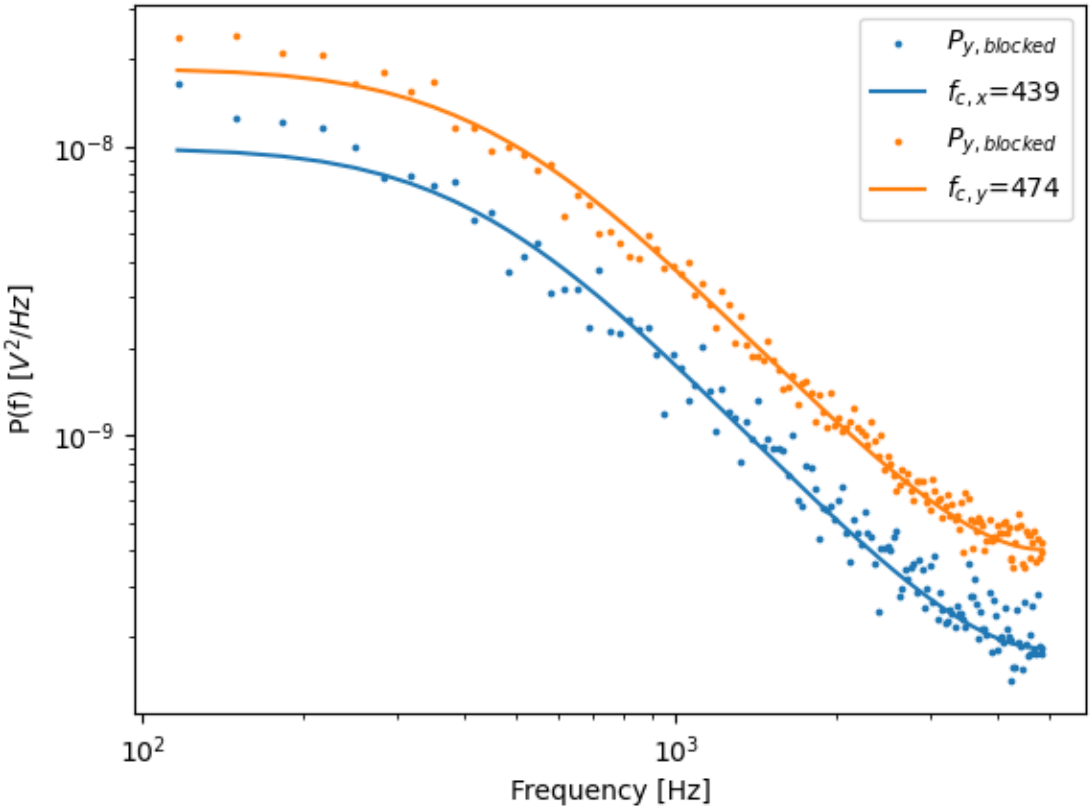

Figure 5.3: Recorded power spectra fitted to eq. **??**, scattered points represents the blocked data ($n_b = 100$). Corner frequency for the Lorentzian curves are reported in the legend.

ratio between the QPD signal and the sphere's position. The corner frequencies and corresponding trap stiffness are reported below:

Table 5.1: QPD fitting for single sphere

Fitting parameter	*ott* estimates		QPD fitting		Trajectory fitting	
$f_c\ [Hz]$	447	450	439	474	523	513
$\sigma(f_c)\ [Hz]$	—	—	9.30	9.65	8.67	8.61
$\kappa\ [pN/\mu m]$	53.05	53.40	51.96	56.09	61.94	60.7
Ellipticity	8.16 %		27.17 %		13.8 %	

Where $\sigma(f_c)$ is computed from [1], where the variance is based upon our choice of frequency boundaries ($f_{min} : f_{max} = 100\ Hz : 5000\ Hz$). And the ellipticity of the beam is given by $e = (1 - \kappa_y/\kappa_x)^{0.5}$ and is a measure of the symmetry of the beam

wavefront. Its clear from these initial results that the QPD is more sensitive to changes along the y-axis than the x-axis when compared to the direct *ott* calculations. This is somewhat reflected in the trajectory results. Typically, even an industrial Gaussian beam will produce an elliptical diffraction limit spot when heavily focused; in their tutorial for optimizing the PSD analysis, Berg and Sorensen reported a ellipticity of around 15 % after a total calibration time of 80 seconds [1].

The reason for the discrepancies between all 3 methods is due to what is actually being measured. The *ott* estimates are simply looking at the change in the trapping force as you move along a given axis'. In reality, a particle will be freely diffusing within the trap focus meaning over a short calibration time the QPD is only estimating a weighted average of the trapping strength. If calibrated over an long enough time frame you would expect that the resulting power spectra would exactly mirror the *ott* predictions. There is a clear trade off in terms of accuracy and computation time as shorter calibration runs are computationally more efficient but prone to errors. However, it should be noted that the estimation made by the QPD is still less than the results from [1], though this could be due to a lack of external noise signals.

With this in mind, let us consider a symmetric dimer that is optically trapped by the same Gaussian beam. Not only does the dimer's equilibrium position change but it is subjected to rotational motion due to its unequal moments of inertia. This is reflected in the calibration results using the simulated QPD, where we see a drastically different estimation between the *ott* estimate and the QPD estimate.

Table 5.2: QPD fitting for symmetric dimer

Fitting parameter	*ott* estimate		QPD fitting		Trajectory fitting	
f_c $[Hz]$	445	409	431	424	274	285
$\sigma(f_c)$ $[Hz]$	—	—	9.22	9.16	7.82	7.91
κ $[pN/\mu m]$	52.82	48.54	51.13	50.26	32.45	33.75
Ellipticity	28.5 %		12.7 %		13.8 %	

Now we see that the *ott* predicts a more elliptical trap compared to the QPD model which says the trap is far more symmetrical while trapping a symmetric dimer. A potential reason that *ott* no longer expects a circular trap is because that unlike a

sphere, the force displacement curve is not strictly harmonic. If we consider a dimer that is some distance from the beam axis, the sphere closest to the trap focus will experience a slightly greater force compared to the sphere further from the trap. As such its not accurate to assume that the external force $F(x) = \kappa x$ instead we must consider that it is a function of both the position and orientation simultaneously.

There is still a concern in the fact that both produce similar power spectra, enough so that it would be difficult to determine if a trapped particle was actually a dimer or a sphere. This is because the rotational and translational motion, coupling of the has been highlighted previously [5], but there effects have not been demonstrated in the context of an experimental situation. We can see from the difference in trajectory and QPD fittings that while our description of the trap shape is very similar (both methods give similar ellipticity values) but the magnitude of the trap strength are significantly different. This is partially explained by the fact that the QPD is not actually measuring the position of the particle but instead the intensity distribution of the total field incident on the QPD surface. In which case if the dimer is rotated slightly the QPD signal will change even if the dimers centre of diffusion remains stationary.

5.4 QPD for angular displacement detection

The next logical step is to consider whether or not a QPD can at all be utilised for detection of rotational motion. This has been shown for nano-particles that exhibit periodic rotational motion using by considering the difference in diagonal quadrants [6]. The only difference between these results is the fact that rotation occurs perpendicular to the particle's long axis, whereas dimers rotate about their long axis. The benefit of detecting rotational motion is that one can begin to build a better understanding about how angular momentum is transferred to a dimer which could be extended to more complex particles. This could give some understanding to the results of Chapter 4.

At just a cursory glance it would appear that there is a clear relationship between the QPD signal and the orientation of the dimer. If we look at the QPD signal produced

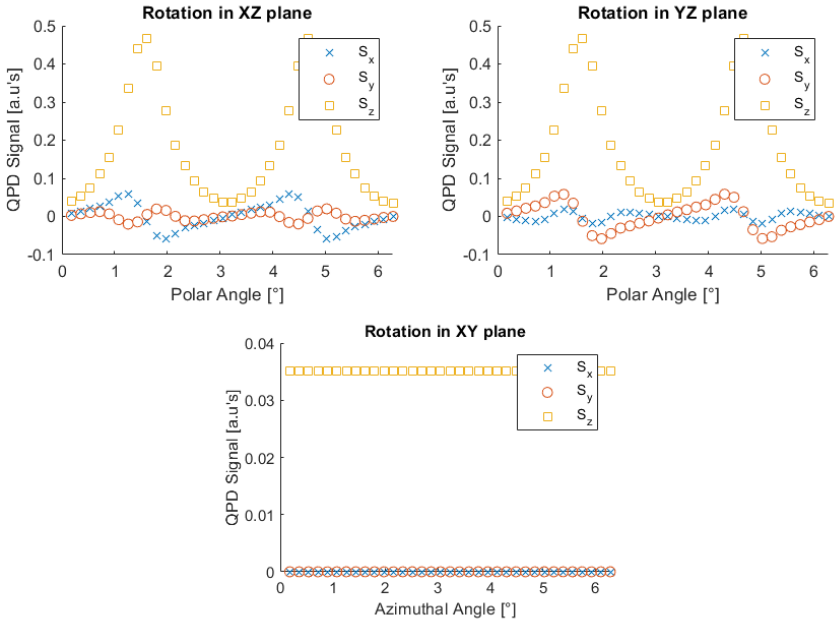

Figure 5.4: QPD signals detected by a dimer being rotated while centred at the focus of the optical trap. Top right: rotation in the X-Z plane. Top left: rotation in the Y-Z plane. Bottom: Rotation in the X-Y plane.

by a dimer as it is rotated we can see that it is equally sensitive to rotations in either the X-Z or Y-Z plane but there is no change in the signal when rotated by in the X-Y plane.

However if we compare this to fig. 5.2 we can see that the the signal change is dwarfed by the translational motion. So while their is a clear relationship between the two trying to discern between translational and rotational contributions to the QPD signal is not a simple task. This is significant because it means that with regards to the power spectrum fittings in Table 5.2 there is no means of discerning between that of a trapped sphere and that of a trapped dimer. Furthermore the dynamics reported by the power spectrum fitting do not accurately reflect the actual dynamics of the dimer, instead only providing a orientation-averaged trap strength. But unless we have some means of at least estimating the degree of rotational freedom, calculating the actual trapping strength is impossible.

The dependence of S_x and S_y and the dimer's orientation (defined by the spherical

angles θ, ϕ) is therefore not clear. To that end, we utilised machine vector regression, which takes as an input the voltage from the 4 quadrants and tries to fit that to the dimer's trajectory. We utilised the scikit-learn module available in Python to transform the 4D vector of the QPD signal to a 2D vector specifying the expected displacement of the target particle. Unlike in Chapter 4 where we utilised machine learning to get a probabilistic estimation of the particle's orientation we utilise vector regression as we want to replicate QPD precision as closely as possible.

In order to fit the QPD signal to dimer displacements we need to train our model. For each size ratio considered a 3 second trajectory was ran (using the same conditions in Sec. 5.3) and a normal distribution of the dimer's position was taken and used to construct a training data set of QPD signals. After the training results reached an error rate of less than 1% the same trajectory was used to construct a test set that would allow our model to fit the QPD signal to the positional data from the trajectory. Fitting the QPD signal to the dimer's position showed promising results, shown in fig 5.4 is a prediction of a symmetric dimer's position based on the QPD signal. With the actual displacement on the x-axis and the predicted result y-axis, and the dashed line represents the y=x line - indicating an ideal prediction.

Fig 5.5 shows that its relatively trivial to predict a particle's position based off the QPD signal in the X-Y plane but harder along the axial direction. If we consider Fig 5.2 we note that the change in signal strength is only truly linear close to the beam focus, as shown in Chapter 3, dimers do not trap close to the beam focus but further away. This would suggest that the model cannot accurately predict the displacement of a dimer in the axial direction as there is a non-linear relationship between the change in signal and the change in axial position. It should be noted that even in the worst case the difference between the predicted and true displacements is around $20nm$.

These displacements are relative to the trap focus and so accurate tracking of the beam movements needs to be taken if you want to consider the displacement relative to some larger object. These results are likely due to the fact that displacement and signal units are linearly related by (5.1). Interestingly when we run the same protocol for different sized dimer's there seems to be a cut off point when the fit begins to fail.

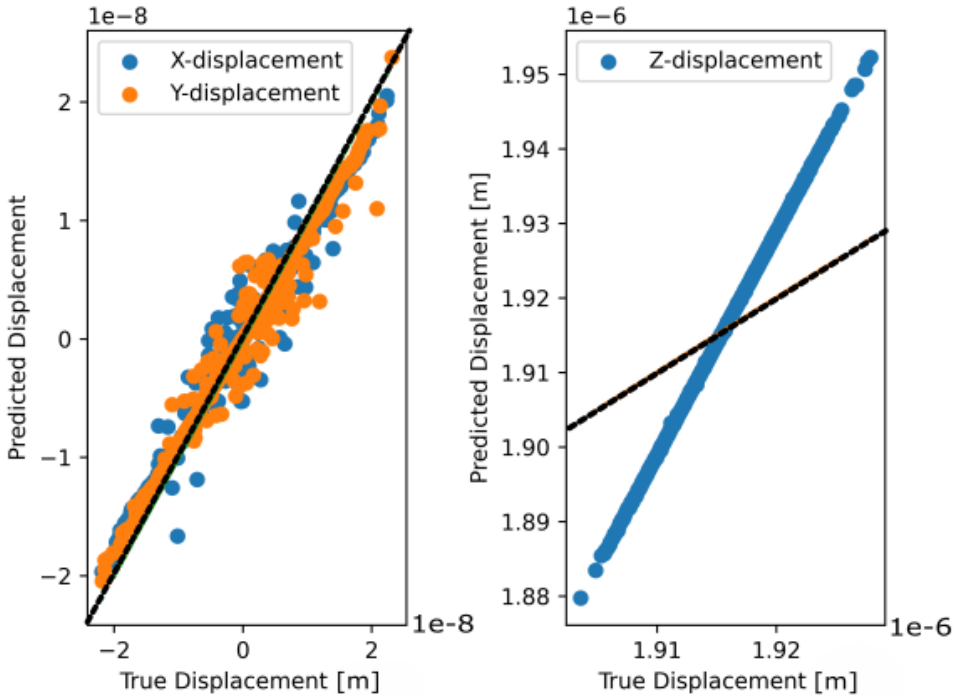

Figure 5.5: Scikit-Learn's best predictions of the displacement of a symmetric dimer placed in an optical trap, predictions are based on the QPD signal collected at the 4 quadrants. (Left) predictions of the X & Y displacements. (Right) predictions of the Z displacement, predictions have been scaled so they represent the displacement from the beam focus. The dashed black line represents when the predicted displacement = the true displacement.

We can compute the coefficient of determination (R^2) for our model's prediction, the R^2 for each fit vs its size ratio shows that beyond a size ratio of 5 the machine learning begins to fall off significantly.

This is surprising because we would expect that as the second sphere shrinks the dynamics should more closely approximate that of a single sphere. This should be reflected in the total field incident on the QPD and therefore the machine learning program should be able to easily detect the dimer's translational motion. We can therefore only conclude that the contribution that the second sphere makes to the scattered beam is not proportional to its size. What is interesting is that the axial prediction does not experience as a large a drop in accuracy, suggesting that the total field incident on the QPD is not changing drastically, but rather that the second sphere

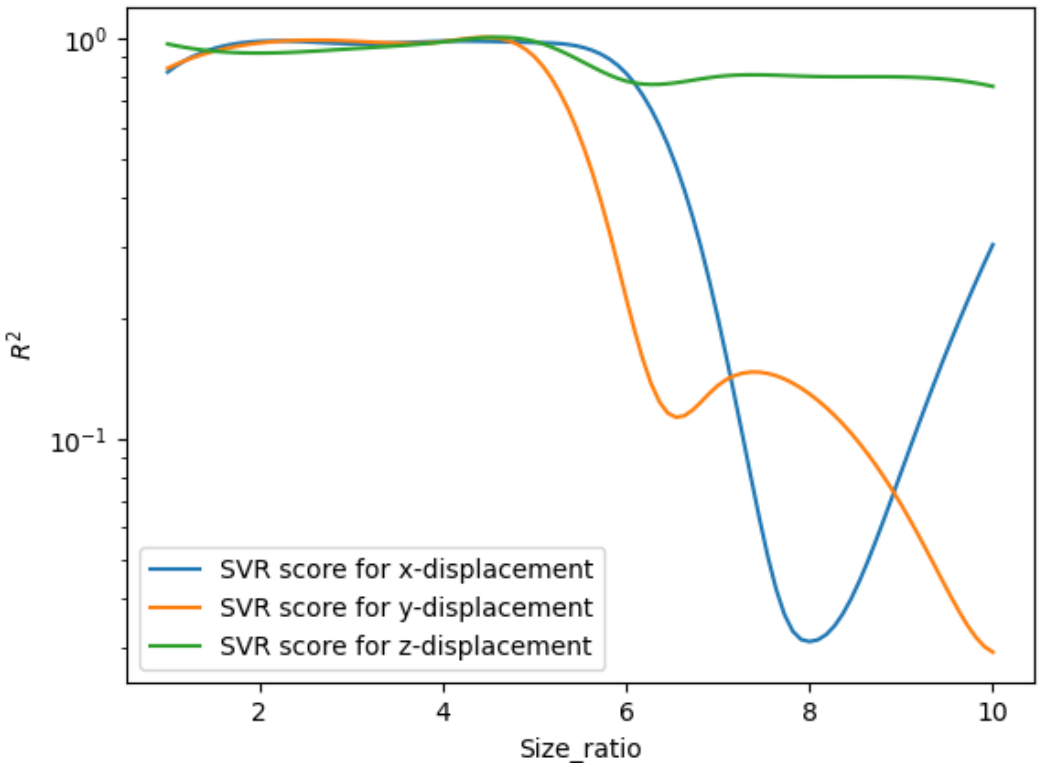

Figure 5.6: The coefficient of determination for different sized dimers using the scikit-learn vector regression model. Each line plot shows the R^2 value for either the X, Y, or Z displacements. When the size ratio is greater than 5 the R^2 value falls off dramatically, from around 0.95 down to as low as 0.01.

is altering the distribution such that the $X - Y$ displacements are being incorrectly predicted. This could simply be a limitation of the *mstm* software being unable to accurately represent the T-matrix of the second sphere, however the documentation does not specify any limits on the relative size differences so it is unclear if this is a known issue. The problem is that it is difficult to verify the error between the *mstm* predicted scattering and the true scattering without replicating the exact system experimentally. For now we can say that predictions for size ratios greater than 5 should be for the most part disregarded.

Detection of rotational motion was attempted using the same method, the model was trained on the same trajectory mentioned in **??**, where the dimer is trapped in an off-axis orientation. We chose this trajectory instead of a strictly vertical orientation

in order to confirm that the model can distinguish between the polar angle and the azimuthal angle. The results of which are are shown in Fig.5.7

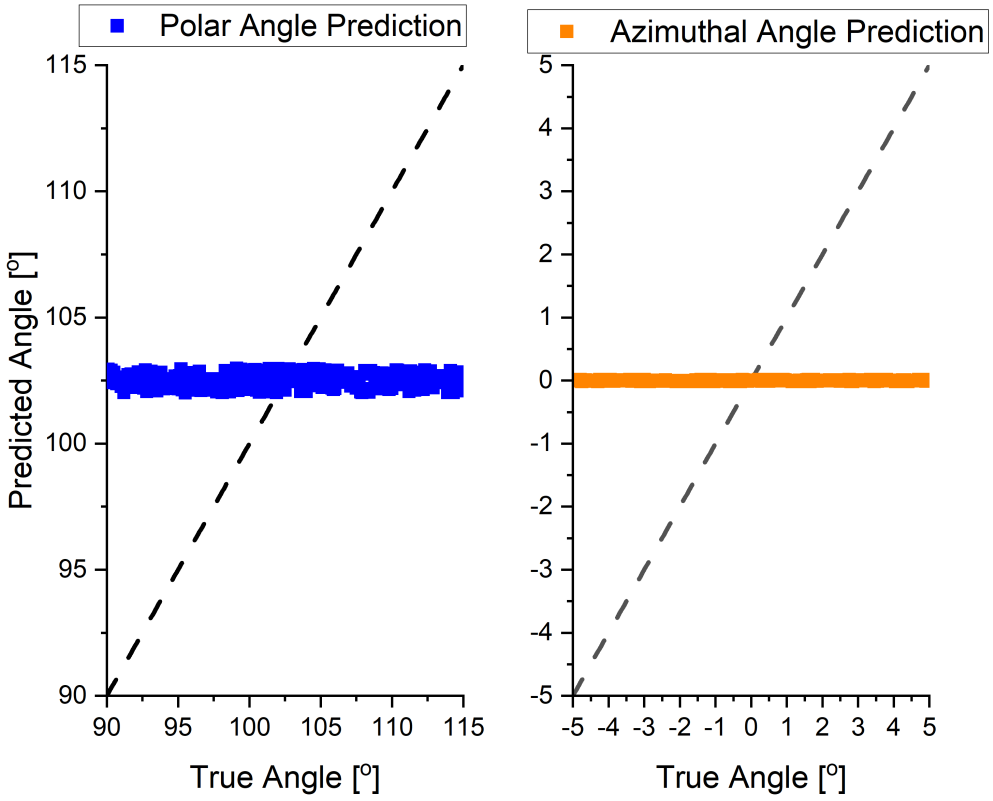

Figure 5.7: Scikit-learn's prediction of the sphericical angles of a dimer trapped in an off-axis configuration (see Sec**??**). (Left) predictions of the azimuthal angle, (Right) predictions of the Polar angle. Dashed black lines show the ideal prerformance where the predicted angle = true angle.

From here we can see that the vector regression model performs rather poorly in predicting the rotations made by the dimer, even in a situation where visibly the dimer is an off-axis orientation. While the model can roughly predict the median polar angle (102 deg) it has no means of predicting the rotations made by the dimer. This result is reveals two important factors: Firstly, the change in the QPD signal for rotational motion is a full order of magnitude smaller than the change in signal for translational motion meaning the model has no means of distinguishing between large and small rotations. Secondly, is the fact that unlike translational motion, rotational motion is

dependent on the prior orientations in the trajectory. This was already discussed in Chapter 4 where we improved our machine learning model by accounting for the the priors $p(\hat{\mathbf{n}}_\alpha)$, where we weighted our estimation by the distance from our prior estimate. Vector regression is powerful for predicting uncorrelated events but has no means for accounting for cases where one event is dependent on the next. At the same time, utilising machine learning in the case of a QPD would not be able to provide a high enough orientational resolution without first sampling from a trajectory and creating a unique set of reference orientations (see Sec. **??** for definitions).

Overall, the reliance on machine learning to perform vector regression on the collected scattered field is not a viable method for detecting let along characterising the angular displacement of an isotropic scatterer. While there is a clear correlation in the scattered signal and angular displacement the translational motion makes up the majority of the expected signal detected by the QPD. As of now, there is no optical arrangement that would allow rotational motion while restricting translational motion.

5.5 Conclusion

We have developed a program that allows one to compute the QPD response signal produced by an arbitrary shaped particle. By utilising *mstm* we can construct any combination of spherical particles and measure the total field incident on the focal plane of the condenser lens. This has immediate applications in replicating power spectral data from complex particle structures that experience periodic rotational motion. Furthermore, if all contributions to the QPD response signal are known it would allow researchers to compare the reported dynamics given by an experimental QPD to that of our simulated response signal.

The QPD module shows promising results for dimers who have a size ratio less than 5. Utilising vector regression models allowed for accurate predictions of the displacements made by dimers while confined by an optical trap. The use of vector regression is necessary to return a continuos range of positions instead of a probabilistic approximation of the particle's position vector.

As shown in 5.4 random rotational motion is difficult to distinguish from random translational motion. Even when utilising a vector regression model the angular displacement predicted does not match the trajectory data. This means that at least for now utilising focal plane interferometry cannot provide an accurate estimation of angular displacements. While static light scattering methods - as seen in Chapter 4 - do present a possible alternative, the limited angular resolution due to a high mixing of signal and orientation spaces also make the method difficult to implement. Measurements of angular displacement are crucial for measuring torques exerted on trapped particles, current torque measurements assume that only the the polarisation contributes to the applied torque, measuring non-polarisation related torques still eludes us.

Overall, tracking the angular displacements of non-spherical objects for the purposes of torque measurements will require further study. Fully understanding the torques applied to an arbitrary shaped particle would pave the way for high-precision particle-manipulation techniques and a greater understanding of the interactions between focused beams and aggregate particles.

Bibliography

[1] Kirstine Berg-Sørensen and Henrik Flyvbjerg. "Power spectrum analysis for optical tweezers". In: 75 (2004), pp. 594–612. ISSN: 0034-6748. DOI: 10.1063/1.1645654.

[2] Lars Friedrich and Alexander Rohrbach. "Tuning the detection sensitivity: a model for axial backfocal plane interferometric tracking". In: *Opt. Lett.* 37.11 (June 2012), pp. 2109–2111. DOI: 10.1364/OL.37.002109. URL: https://opg.optica.org/ol/abstract.cfm?URI=ol-37-11-2109.

[3] Graham M. Gibson, Jonathan Leach, Stephen Keen, et al. "Measuring the accuracy of particle position and force in optical tweezers using high-speed video microscopy". In: *Optics Express* 16.19 (Sept. 2008), p. 14561. ISSN: 1094-4087. DOI: 10.1364/oe.16.014561.

[4] Alexander Rohrbach and Ernst H. K. Stelzer. "Three-dimensional position detection of optically trapped dielectric particles". In: *Journal of Applied Physics* 91.8 (Apr. 2002), pp. 5474–5488. ISSN: 1089-7550. DOI: 10.1063/1.1459748.

[5] Wyatt Vigilante, Oscar Lopez, and Jerome Fung. "Brownian dynamics simulations of sphere clusters in optical tweezers". In: *Optics Express* 28.24 (Nov. 2020), p. 36131. ISSN: 1094-4087. DOI: 10.1364/oe.409078.

[6] Yuval Yifat, John Parker, Tian-Song Deng, et al. "Facile Measurement of the Rotation of a Single Optically Trapped Nanoparticle Using the Diagonal Ratio of a Quadrant Photodiode". In: *ACS Photonics* 8.11 (Nov. 2021), pp. 3162–3172. ISSN: 2330-4022. DOI: 10.1021/acsphotonics.1c00802.